

OPTICAL BEAM LOSS MONITOR INSTALLED AT THE SPS SLOW EXTRACTION REGION

M. King^{*1}, S. Benitez Berrocal, E. Effinger, J. Esteban, J. Kearney, J. M. Meyer, B. Salvachua
CERN, Geneva, Switzerland

C. P. Welsch¹, J. Wolfenden¹, Cockcroft Institute, Daresbury, United Kingdom

¹also at University of Liverpool, Liverpool, United Kingdom

Abstract

An optical beam loss monitor (oBLM) has recently been installed at the slow extraction region of the Super Proton Synchrotron (SPS) at CERN. The oBLM offers a new method for detecting beam losses at the SPS by utilizing the Cherenkov radiation emitted during beam loss interactions with an optical fibre. This setup should allow to measure losses continuously over a large section of the accelerator, thus minimising the non-linearities caused by the finite coverage of the currently installed ionisation chambers. Due to the high radiation levels and low expected signals at this location, special care was taken during the procurement process to maximise the signal levels while at the same time extending the lifetime of the system as much as possible. The rationale behind the choice of specific components is discussed, highlighting their advantages compared to other options. Furthermore, initial measurements of beam loss during extraction are presented, and the system's ability to provide real-time diagnostics for machine protection and beam optimization investigated.

INTRODUCTION

The Super Proton Synchrotron (SPS) at CERN not only delivers high-intensity proton beams to the LHC, but also to a variety of other experiments, including fixed target experiments in the North Area. The beams toward the North Area are extracted over several seconds using a slow extraction technique based on a third-order resonance, a method that is inherently lossy [1, 2].

To monitor these losses and support safe and efficient operation, the SPS operators rely on a number of ionisation chamber (IC) beam loss monitors (BLMs) installed in this region. However, conventional IC-BLMs provide limited spatial coverage. Therefore, when using the beam loss signals to optimize the machine, it cannot be distinguished between a local reduction of beam losses or a shift of beam losses to an area that is not covered by the IC-BLMs system.

The need for a longitudinal BLM has been expressed as a solution to improve the longitudinal coverage of the beam loss monitoring during the slow extraction [3]. It was chosen to pursue optical BLMs (oBLMs) as the primary option for this region. oBLMs have been investigated at multiple facilities around the world [4–9] and recently at CERN at the CERN linear electron accelerator for research (CLEAR) [10, 11]. oBLMs are based on Cherenkov light

being emitted when charged loss particles traverse optical fibres at a high speed. The optical fibre not only detects the loss particles but can also transport the emitted Cherenkov photons to either end of the fibre at which photodetectors are located. This enables position-resolved monitoring over long distances. Previous installations have typically been at accelerators with low beam repetition rates and clear bunch structures. This allows to use the timing information of the loss signals to reconstruct the loss position.

However, using oBLMs to cover the SPS slow extraction region presents a unique combination of challenges not encountered in earlier test campaigns at CLEAR or other installations. These include high radiation levels, the absence of time structure within the unbunched beam, a lack of shielding for the photodetectors, and the relatively large distance between the fibre duct and the beam due to integration restrictions.

In the following, decisions taken during the procurement process to minimise the impact of these issues will be discussed and preliminary results will be shown.

INSTALLATION

For this installation, three main choices had to be made. What type of optical fibre to use, which photodetectors are best suited to these conditions and how to readout the data.

Optical Fibre

Through simulations and a previous prototype [12], it quickly became clear that it would be vital to increase the signal capture as much as possible. Therefore, instead of the 200 μm , 0.22 numerical aperture (NA) fibre previously installed, it was decided to install a 600 μm , 0.5 NA, high hydroxyl group (OH) concentration optical fibre, FP600URT from “Thorlabs, Inc.”. By choosing a thicker fibre, both the area covered by the oBLM and the mean path length of particles hitting the fibre is increased. This leads to a noticeable increase in captured signal. Simulations indicate that signal levels increase with the thickness of the fibre to the power of 2.5 [12]. This results in an increase of a factor of 15.6 when comparing between these two fibres.

Increasing the NA increases the angular range in which photons are captured and transported along the fibre, as visualised in Fig. 1. The curves were calculated based on formula (22) in [13]. This comes at the cost of higher dispersion [6]. Going from a NA of 0.22 to a NA of 0.5 increases the overall captured signal by a factor of 5.42, assuming a uniform angular distribution of loss particles. This is calculated by

^{*} m.king@cern.ch

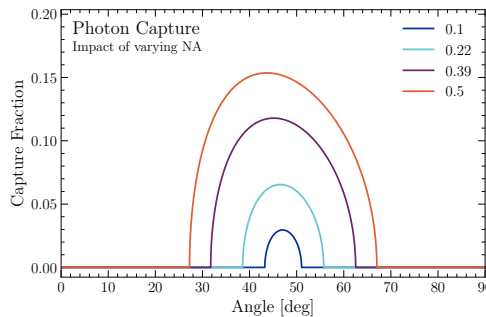


Figure 1: Calculated fraction of captured Cherenkov photons as a function of loss particle angle to the optical fibre for different numerical apertures. The speed of the particle is assumed to be approximately the speed of light in vacuum.

integrating over the respective curves shown in Fig. 1. Together, these two effects increase the expected signal levels by a factor of approximately 85 when compared to the fibre initially installed.

High OH fibres tend to be slightly more radiation tolerant than low OH fibres at high wavelengths [14]. With radiation levels of up to 200 kGy per year close to the beam line, radiation induced attenuation is expected to be noticeable on the time scale of months. Nevertheless, research into even more radiation tolerant fibres is ongoing.

To cover the entire 200 m length needed to monitor the SPS slow extraction area, two 100 m long fibres were used, connected with FC/PC connectors. While longer optical fibres with these thicknesses exist, these break when putting on protective tubing any longer than 100 m due to the mechanical stresses involved in this process. Due to restrictions by other systems along the extraction region, these were pulled through a plastic fibre duct which was installed at a distance of 2.4 m to the beamline.

Photodetectors

The main criteria used to select suitable photodetectors were their radiation hardness due to the harsh environment encountered at the SPS [2]. This immediately excluded Silicon Photomultipliers and left Photomultiplier Tubes (PMTs) as the only viable option [15]. The main way PMTs are affected by radiation is through browning of the window material [16]. Often borosilicate glass is used which shows a significant reduction in low wavelength transmission after irradiation of a few thousand Gray [16]. Silica glass, on the other hand, only starts to show very slight browning effects after tens of thousands of Gray making it the premier choice for the PMT window material for this use case [16].

However, silica windows are typically only used in combination with low wavelength photocathodes. While Cherenkov radiation follows a $1/\lambda^2$ distribution, seemingly making this ideal, these low wavelengths are highly attenuated by the optical fibre. In practice, oBLMs typically use high wavelength (600 nm to 900 nm) photodetectors to reduce the impact of signal attenuation within the fibre as

much as possible. After an extensive market research, it was found that this combination does not commercially exist. Therefore custom made PMTs of the R9880 series by Hamamatsu were procured, using a silica window in combination with the “-20, Extended red Multiakali” high wavelength sensitive photocathode. These were first tested at an oBLM installation at CLEAR [11] before being installed at the SPS.

A PMT was attached to each side of the fibre. The downstream end of the fibre was led an additional 2 m away from the beamline to reduce the amount of beam losses impacting the PMT. For the upstream PMT this was not possible but also not necessary due to the lower radiation levels.

Readout

To readout and save the data, it was decided to install a PicoScope 6426E with a 1 GHz bandwidth at the surface, connected to both readouts via CK50 cables. This was connected to CERN’s internal technical network and allowed for remote control and automatic operation with python scripts. Multiple such data taking scripts were written to be able to investigate different timescales of the oBLM signals. The main difficulty of data taking is that the duration of single signal peaks is approximately ten nanoseconds whereas the extraction takes roughly 5 s. This means that either single signals cannot be resolved or only part of the extraction can be analysed and saved due to the extreme amounts of data necessary to do both at the same time. This setup gives sufficient flexibility to study the signal patterns. In the future, the PicoScope will potentially be replaced with custom solutions able to incorporate on-the-fly processing of the data.

RESULTS

Figure 2 shows the waveforms measured during extraction. The signal is measured as a negative voltage. To increase the signal-to-noise ratio, the up-and downstream signals were averaged over 43 extractions. These 43 extraction cycles correspond to a measurement time of approximately 30 min. One can clearly identify that the data taking starts 2 s before the start of the extraction. This is then followed by an approximately constant, 5 s negative signal pulse, which agrees with the length and structure of the extraction. Despite being averaged over multiple waveforms, the signal is relatively noisy. This is due to the high sampling interval of 100 μ s without any other signal smoothing electronics (compared to the single signal peak duration of the order of ns).

Averaging the downstream oBLM signals sampled at a rate of 1 MHz over the 5 s extraction duration and comparing these measurements to the sum of the IC-BLMs in the region over time gives Fig. 3. This plot shows extraction loss data taken over ten days and overall a very good agreement between the oBLM and IC-BLMs is visible. The upstream oBLM gives similar results. One can, however, see some peaks in the ratio between the two BLM types which typi-

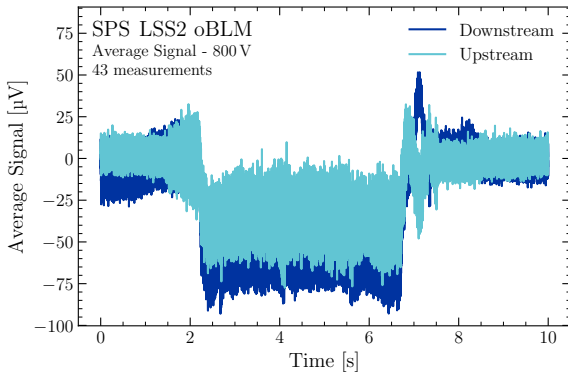


Figure 2: Full extraction averaged over multiple extractions for both the up- and downstream readout. A sampling interval of $100\text{ }\mu\text{s}$ was used. One can clearly identify the trigger set to two seconds before extraction start and the extraction causing increased beam losses at a constant rate during the entire extraction for the following 5 s.

cally correspond to low signal extractions. These low signal levels indicate low beam intensity which is mainly used during accelerator machine development which likely leads to different loss patterns. The ratio of the upstream oBLM to the IC-BLMs shows dips at the same locations. This could indicate that the beam losses are shifted toward the downstream readout in these cases. This effect is complicated by the layout of the IC-BLMs. As the main loss areas are expected close to the upstream end of the fibre, this is also where the majority of IC-BLMs were installed. This limited coverage of losses downstream results in a non-linear weighting of beam losses when simply using the sum of all signals. A loss event near the upstream end could induce a signal in multiple IC-BLMs whereas the same loss shower further downstream might only be detected by a single IC-BLM, leading to a much lower signal overall. Different methods to compensate for this effect are currently under investigation.

Finally, measurements with a high sampling rate of 1.25 GHz were conducted. Due to aforementioned restrictions, this results in a total measurement time of 0.8 ms and therefore a delay of 3.2 s is used relative to Fig. 2 to ensure the measurement takes place during the extraction. This allows to investigate the behaviour of single loss signals as shown in Fig. 4. This plot shows a $2\text{ }\mu\text{s}$ time window of the total measured waveform. In this case, one can see both an upstream and a downstream signal pulse. Assuming these come from the same loss event, one could use this difference in time combined with knowledge of the length of the optical fibre to reconstruct a loss position. However, in practice, only few upstream signals have clearly identifiable downstream signals within the expected time window. It is not yet clear if this is mainly due to the low capture rate of losses or rather if this is only a statistical effect. These signals could instead stem from different loss events which only per chance lead to signals within the same time window. Long duration measurements are ongoing and the resulting reconstructed

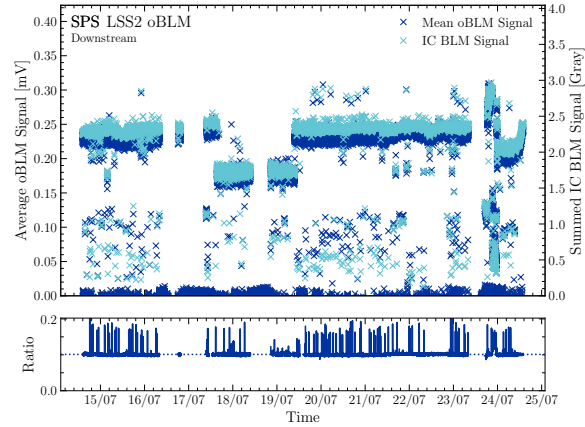


Figure 3: Downstream oBLM signal, dark blue, averaged over the extraction duration as a function of time. In light blue, the summed signal over all IC-BLMs in the region covered by the oBLM. For easier comparison, the ratio of the oBLM/IC-BLM is also shown in the bottom plot.

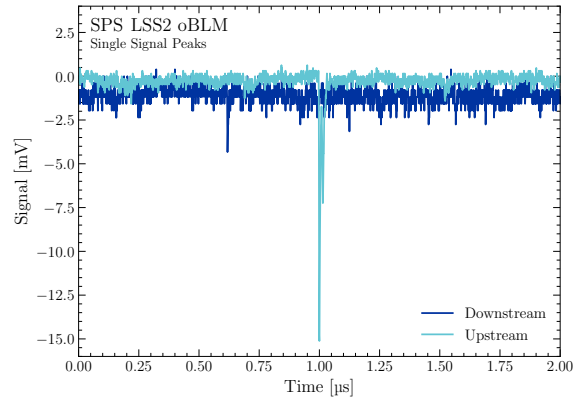


Figure 4: Downstream, light blue, and upstream, dark blue, signal measured during extraction. The sampling interval is $1\text{ }\text{ns}$ and the plot width is $2\text{ }\mu\text{s}$. The offset compared to the trigger used in Fig. 2 is approximately 3.2 s.

loss distribution should allow to tell whether the origin of these signal pairings is correlation or coincidence.

CONCLUSION

While the slow extraction region of the SPS presents a highly challenging environment for beam instrumentation in general, a working prototype oBLM has been installed and beam loss data successfully recorded. A thorough investigation and optimisation is still ongoing, but preliminary results are highly promising. The average oBLM signals over an entire extraction agree well with the IC-BLMs in the region during normal operations, both up- and downstream. Furthermore, while standard loss position reconstruction techniques are not applicable to this installation, investigations into novel reconstruction techniques are ongoing.

REFERENCES

- [1] F. M. Velotti *et al.*, “Characterisation of the SPS slow-extraction Parameters”, in *Proc. IPAC’16*, Busan, Korea, May 2016, pp. 3918–3921.
doi:10.18429/JACoW-IPAC2016-THPOR055
- [2] M. A. Fraser *et al.*, “Slow extraction efficiency measurements at the CERN SPS”, in *Proc. IPAC’18*, Vancouver, Canada, Apr.-May 2018, pp. 834–837.
doi:10.18429/JACoW-IPAC2018-TUPAF054
- [3] M. A. Fraser *et al.*, “Upgraded beam instrumentation for slow extraction at SPS”, CERN, Tech. Rep. EDMS-2113420, 2019.
- [4] E. Janata and M. Körfer, “Radiation detection by Cerenkov emission in optical fibers at TTF”, DESY, Tesla Report 2000-27, 2000.
- [5] P. J. Giansiracusa *et al.*, “A distributed beam loss monitor for the Australian Synchrotron”, *Nucl. Instrum. Methods Phys. Res. A*, vol. 919, pp. 98–104, 2019.
doi:10.1016/J.NIMA.2018.12.054
- [6] Y. I. Maltseva and V. G. Prisekin, “Optical fiber based beam loss monitor for the BINP e-e+ injection complex”, in *Proc. RuPAC’18*, pp. 486–488, 2018.
doi:10.18429/JACoW-RUPAC2018-THPSC38
- [7] S. V. Cao and M. L. Friend, “Investigation of an optical-fiber based beam loss monitor at the J-PARC extraction neutrino beamline”, in *Proc. IBIC’20*, pp. 110–113, 2020.
doi:10.18429/JACoW-IBIC2020-WEPP06
- [8] A. S. Fisher *et al.*, “Beam-loss detection for the high-rate superconducting upgrade to the SLAC Linac Coherent Light Source”, *Phys. Rev. Accel. Beams*, vol. 23, no. 8, p. 082802, 2020. doi:10.1103/PhysRevAccelBeams.23.082802
- [9] J. Wolfenden *et al.*, “Cherenkov radiation in optical fibres as a versatile machine protection system in particle accelerators”, *Sensors*, vol. 23, no. 4, 2023. doi:10.3390/s23042248
- [10] S. Benítez, B. Salvachúa, and M. Chen, “Beam loss detection based on generation of Cherenkov light in optical fibers in the CERN Linear Electron Accelerator for Research”, *Phys. Rev. Accel. Beams*, vol. 27, no. 5, p. 052901, 2024.
doi:10.1103/PhysRevAccelBeams.27.052901
- [11] M. King *et al.*, “A systematic investigation of beam losses and position-reconstruction techniques measured with a novel oBLM at CLEAR”, *Instruments*, vol. 9, no. 1, 2025.
doi:10.3390/instruments9010004
- [12] S. Benítez, “Design and development of an optical beam loss monitor based on Cherenkov light detection for the CERN Super Proton Synchrotron accelerator”, Ph.D. dissertation, University of Huddersfield, Queensgate, UK, 2022.
- [13] S. H. Law, S. C. Fleming, N. Suchowerska, and D. R. McKenzie, “Optical fiber design and the trapping of Cerenkov radiation”, *Appl. Opt.*, vol. 45, no. 36, pp. 9151–9159, 2006.
doi:10.1364/AO.45.009151
- [14] S. Girard *et al.*, “Radiation effects on silica-based optical fibers: Recent advances and future challenges”, *IEEE Trans. Nucl. Sci.*, vol. 60, no. 3, pp. 2015–2036, 2013.
doi:10.1109/TNS.2012.2235464
- [15] A. Ghassemi, K. Sato, and K. Kobayashi, *Technical guide to silicon photomultipliers (MPPC)*, Hamamatsu Photonics K.K., Hamamatsu Photonics K.K., 2022. https://www.hamamatsu.com/content/dam/hamamatsu-photonics/sites/documents/99_SALES_LIBRARY/ssd/mppc_kapd9005e.pdf
- [16] *Photomultiplier tubes basics and applications*, Hamamatsu Photonics K.K., 2017.